Journal of Asian Earth Sciences 220 (2021) 104936

Contents lists available at ScienceDirect

Journal of Asian Earth Sciences

journal homepage: www.elsevier.com/locate/jseaes

Importance of real-time PGV in terms of lead-time and shakemaps: Results using 2018 M_L 6.2 & 2019 M_L 6.3 Hualien, Taiwan earthquakes

Himanshu Mittal[a,b,1], Benjamin Ming Yang[b], Tai-Lin Tseng[b], Yih-Min Wu[b,c,d,*]

[a] Amity Center of Ocean-Atmospheric Science and Technology (ACOAST), Amity University, Jaipur, Rajasthan 303002, India
[b] Department of Geosciences, National Taiwan University, Taipei 10617, Taiwan
[c] Institute of Earth Sciences, Academia Sinica, Taipei 11529, Taiwan
[d] Research Center for Future Earth, National Taiwan University, Taipei 10617, Taiwan

ARTICLE INFO

Keywords:
Earthquake
Early warning
Peak ground acceleration
Peak ground velocity
P-Alert
Shakemaps

ABSTRACT

Two earthquakes having almost the same magnitude occurred in the Hualien area of Taiwan in 2018 and 2019. The 2018 earthquake had a magnitude M_L 6.2 produced severe destruction; however, the 2019 earthquake (M_L = 6.3) did not cause any severe damage. The P-Alert Strong Motion Network provides real-time shakemaps, in addition, to earthquake early warning (EEW) in terms of lead-time. Each instrument provides a different lead-time using peak ground acceleration (PGA) and peak ground velocity (PGV). During both the events, the instruments reported a lead-time of 1.5 to 8.0 s in the epicentral region. This network system also generated high-quality shakemaps during both earthquakes. The shakemaps showed that the higher PGAs are concentrated in the epicentral region for the 2018 and 2019 earthquakes. The lower PGA contour (≥25 Gal) extended to a broader area, including Taipei, during the 2019 earthquake compared to the 2018 earthquake. However, PGV shakemaps display a different pattern. The higher PGV values (more than 17 cm/s) are observed in the epicentral region during the 2018 earthquake (locations suffering building collapse) compared to the 2019 earthquake, suggesting that PGV correlates better with damage distribution as compared to the PGA. The PGV shakemap, currently only available for the P-Alert network, provides crucial information that complements the PGA issued by the official agency in Taiwan.

1. Introduction

Being located on the junction of two tectonic plates, Taiwan Island is one of the seismically active areas in the world. The Philippine Sea plate (PSP) moves toward the Eurasian plate (EP) at a velocity of approximately 7 cm/year (Yu et al., 1997). Due to the collision of these two plates, the accumulated stresses are released, causing earthquakes in and around Taiwan Island. In addition to this collision, several other local faults in western and southern Taiwan are also responsible for the frequent earthquake activity in Taiwan. Taiwan Island has a long history of earthquakes. The largest recorded earthquake in the last two decades is the Chi-Chi earthquake of September 21, 1999, which claimed more than 2400 lives (Wu et al., 2004). The Nantou earthquakes of 2013 caused few damages in the Nantou area, Taiwan, claiming fewer lives (Hsieh et al., 2014). The recent earthquakes of 2016 caused widespread damage in southern Taiwan (Wu et al., 2016). The 2016 earthquake with a magnitude M_L 6.4 occurred at a depth of 16.7 km and claimed 117 lives. All these earthquakes were caused by the active seismic faults in western and southern Taiwan.

Hualien area, on the contrary, is situated in eastern Taiwan, where earthquake activity is due to the oblique subduction of the PSP under the EP (Koulakov et al., 2014; Shyu et al., 2011). The collision of these two plates gives rise to numerous earthquakes in the Hualien area (Shyu et al., 2016), some of which have a magnitude greater than 4. The major reverse fault, namely, the Milun fault located on the western boundary of the Milun tableland, is mapped in this region (Fig. 1). This Milun fault had been quiet for the last two decades since the massive earthquake struck Hualien in 1951 (Shyu et al., 2005). In recent times, two moderate magnitude earthquakes, namely February 6, 2018 (M_L 6.2) and April 18, 2019 (M_L 6.3), occurred again in this region. The earthquake of 2018 caused significant damage in the epicentral region compared to the earthquake of 2019, although the magnitude of the 2019 earthquake

* Corresponding author at: Dept. Geosciences, National Taiwan University, No. 1, Section 4, Roosevelt Road, Taipei 10617, Taiwan.
E-mail address: drymwu@ntu.edu.tw (Y.-M. Wu).
[1] Presently at National Center for Seismology, Ministry of Earth Sciences, Lodhi Road, New Delhi 110003, India.

https://doi.org/10.1016/j.jseaes.2021.104936
Received 13 August 2020; Received in revised form 19 August 2021; Accepted 22 August 2021
Available online 1 September 2021
1367-9120/

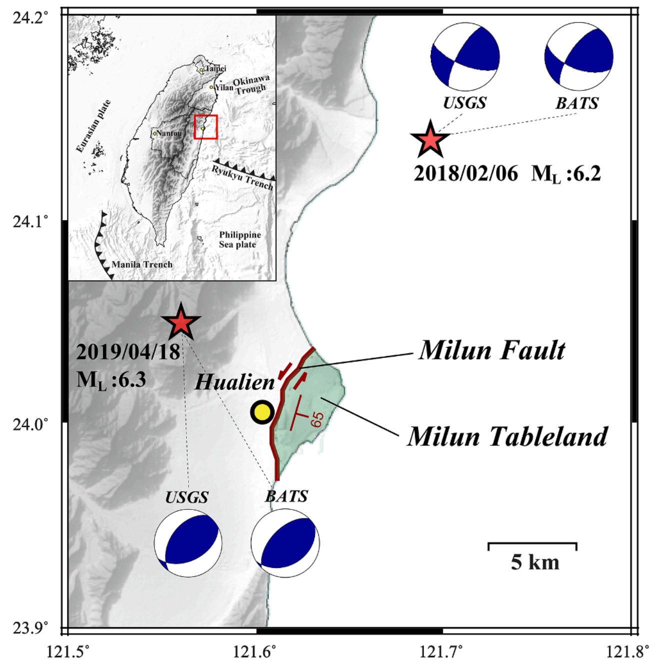

Fig. 1. Tectonics of Taiwan and various faults in the proximity of the Hualien region. The stars depict the locations of the 2018 and 2019 earthquakes. The focal mechanism of both earthquakes by Broadband Array in Taiwan (BATS) and the United States Geological Survey (USGS) is shown.

was higher than in 2018.

Taiwan is one of the regions where earthquake early warning (EEW) is in an advanced stage (Chen et al., 2017, 2015; Wu et al., 1999, 1998; Wu and Teng, 2002). Central Weather Bureau (CWB) is the official agency in Taiwan to issue regional EEW warnings based on real-time data from approximately 120 strong-motion instruments. These strong-motion stations are distributed throughout Taiwan, in an area of 100×300 km^2. Each station has three-component force-balanced accelerometers. The real-time data from field instruments are transferred and processed at the central station in Taipei using Earthworm software (Chen et al., 2015), where the warning is decided based on threshold values. As this process takes 10–12 s, the warning is possible only for areas beyond 50 km from the epicenter, and this 50 km area is termed a blind zone. In these areas, the on-site warning using data from a single instrument may be helpful. Two on-site EEW networks by the National Center for Research in Earthquake Engineering (NCREE) and National Taiwan University (NTU) are operational in Taiwan (Hsu et al., 2018; Wu, 2015; Wu et al., 2013). Since the NCREE network is in the developing stage, we utilize the EEW of the NTU network only in this study. It consists of around 761 low-cost Micro-Electro-Mechanical System (MEMS) based P-Alert instruments. Each P-Alert device is equipped with a three-component accelerometer having 16 bits resolution and $\pm$ 2 g full dynamic range. The sampling rate is 100 samples per second. As per the software algorithm embedded in P-alert, the signal at each field station itself is processed to detect P-wave arrivals and is continuously double-integrated into the displacement signal for calculating the vertical peak amplitude of displacement from the P-wave, P_d. This instrumentation is capable of providing on-site and regional warnings in addition to shakemaps generation. The P-Alert network provides 2 to 8 s on-site warnings at different locations in Taiwan (Wu et al., 2016, 2019). For the regional EEW purpose, the data from the field stations is streamed continuously to the central station at Taipei, where the data is processed to estimate the threshold parameters using the Earthworm software. Because of a large number of instruments, this network provides dense peak ground acceleration (PGA) and peak ground velocity (PGV) shakemaps within two minutes of the occurrence of an earthquake. Before 2019, this instrumentation was used to provide only near real-time PGA shakemaps. With advancements in algorithms, now this instrumentation provides both PGA and PGV shakemaps in real-time. The shakemaps start plotting as soon as an earthquake initiates. This dense network of instruments is possible because of the cost of P-Alert, which is around one-tenth of the usual accelerographs.

P-Alert instruments are in demand in developing countries located at plate boundaries and are at high seismic risk. Many countries, including India (Kumar et al., 2014, 2020), China, Indonesia, Korea, Vietnam, Mexico, New Zeeland, the Philippines, Nepal, Bhutan, and the Solomon Islands, installed P-Alert networks for EEW and risk mitigation. Mittal et al. (2019b) used the recorded P-Alert data from Taiwan to test the functionality of EEW from earthquakes occurring in the Himalayan region, India, a region prone to high seismic activity (Mittal et al., 2016, 2015).

P-Alert network of Taiwan performed very well during the 2018 and 2019 earthquakes. An on-site warning of 1.5 to 8 s was issued during the 2018 earthquake and shakemaps were available within 2 min of the occurrence of the earthquake. Wu et al. (2019) discussed the working of this network during the 2018 earthquake. Another earthquake of 2019 was also well detected by this network, and high-quality data was produced in addition to shakemaps generation. We are motivated by the fact that the earthquake of 2018 (M_L 6.2) caused massive damage in Hualien near the Milun fault as compared to the earthquake of 2019 (M_L 6.3), although the magnitude of the two earthquakes was comparable. The initial rupture during the 2018 earthquake started from a north–south striking fault, propagated to the south with a high rupture speed, and then jumped to the Milun fault. The 2019 event also could be linked with the same fault system that ruptured northward (Lee et al., 2020). In this paper, we examine the data recorded by the P-Alert network during the 2018 and 2019 earthquakes in the Hualien area to study the difference and similarities between PGA and PGV shakemaps produced by the network.

2. The 2018 Hualien earthquake

February 6, 2018, the Hualien earthquake (Ma and Wu, 2019) with M_L 6.2 is caused by the Milun fault. The idea speculating the Milun fault responsible for the 2018 earthquake is the tectonic position of the Milun fault, which is mapped as a reverse fault with the strike-slip component (Shyu et al., 2016). The CWB rapid-reporting system (Wu et al., 1997, 2002) located the earthquake 18 km northeast of the Hualien with a focal depth of 10 km and M_L 6.2. The United States Geological Survey (USGS) and the Broadband Array in Taiwan (BATS) estimated moment tensor solutions, and both of these agencies confirmed the oblique-slip faulting focal mechanism, consistent with the Milun fault (Fig. 1). The 2018 earthquake caused widespread destruction (Yen et al., 2019) in the epicentral region and neighboring areas. Around 17 fatalities were reported during the earthquake. Most of the casualties were associated with a multi-storied hotel building, which tilted due to the collapse of the lower floors. Five other buildings were severely damaged, including a 6-story apartment building, a 9-story apartment building, and an 11-story hotel. Several other buildings suffered structural and non-structural damages (Lin et al., 2020). The Milun fault was thought to be responsible for this earthquake because most of the damage occurred in structures nearby the fault. The PGA during this earthquake reached 600 Gal, which is equivalent to a seismic intensity of VII (the maximum intensity scale in Taiwan).

3. The 2019 Hualien earthquake

On April 18, 2019, an earthquake with M_L 6.3 occurred close to Hualien. According to the CWB rapid-reporting system, the earthquake was located 10 km northwest of the Hualien area with a focal depth of 18.8 km and M_L 6.3. The earthquake was severe to cause panic in residents as the PGA reached 500 Gal, with seismic intensity VII. Because this earthquake occurred during the daytime, many schools were evacuated, keeping in mind the safety of children. Though the considerable PGA (500 Gal) was recorded during this earthquake, only slight structural damage was caused to a few vulnerable buildings. In addition to minor structural damage in the epicentral region, one of the multi-storied buildings in Taipei (around 120 km away) leaned against its neighbor after its foundation shifted. However, no casualties were reported during this earthquake. The earthquake was located by the USGS, as well as, BATS and both of them confirm the reverse focal mechanism with the less strike-slip component as compared to the 2018 earthquake. The primary nodal plane runs from the northeast to the southwest, while the other plane runs from the northwest to the southeast (Fig. 1). This earthquake is also supposed to be caused by the Milun fault because of its focal mechanism and closeness to the fault. This earthquake occurred precisely 14 months after the 2018 earthquake, which caused massive destruction in the epicentral region. Although the PGA experienced during the 2019 earthquake was almost equal to the 2018 earthquake, the structural damage caused by the 2019 earthquake was significantly less or negligible than the 2018 earthquake.

4. P-Alert network and on-site EEW warning

In collaboration with one private company, the NTU research team introduced a low-cost MEMS-based seismic instrumentation network in Taiwan. Being low in cost, these instruments became prevalent in instrumenting Taiwan densely, which was not possible with traditional accelerographs. This instrumentation in Taiwan performs very well for EEW (on-site and regional) and shakemaps plotting. Encouraged by the performance of the P-Alert instruments, many countries, including India, China, Indonesia, and others, are building EEW in their countries using P-Alerts from Taiwan. The earlier version of P-Alert was not promising in dynamic range and storage; however, the second generation of P-Alert instruments has overcome this problem. In Taiwan, P-Alert instruments were installed for the first time in the Hualien area (Wu and Lin, 2014), which faces many earthquakes every year, being situated close to the subduction of the EP and the PSP. At present, 761 P-Alert instruments are installed densely (every 5 km) in different parts of Taiwan Island (Fig. 2). Most of the instruments are installed in school buildings where adequate power supply and internet connection are available, which are the two basic requirements guaranteeing the proper functioning of these instruments. The successful working of the P-Alert network during various earthquakes is documented previously (Wu et al., 2013, 2016, 2019; Wu, 2015). As instruments are installed in two or three-story buildings and on vertical walls, the site effects and sensor-building interaction may affect the recorded PGA. To quantify the difference in PGA values recorded by P-Alert instruments, Wang et al. (2018) collected data from Taiwan Strong Motion Instrumentation Program (TSMIP) operated by CWB, where P-Alert instruments were in the vicinity. They calculated the difference in P-Alert and TSMIP values by dividing the PGA values recorded by both instrumentations (defined as R-value) and proposed that the R-value was one for the P-Alert instruments located on the ground floor. However, the instruments' R-value at the first and second floor was 1.07 and 1.52 times, respectively. This instrumentation performed very well during both the 2018 and 2019 earthquakes and provided high-quality data.

Each instrument in the field acts as an on-site EEW device. The data received in the field by each instrument is double-integrated continuously to calculate the peak vertical displacement value (P_d). The P_d calculation is a two-stage process, where a high pass 0.075 Hz filter is applied to remove the noise content. An on-site warning is issued once the predefined thresholds are exceeded ($P_d \geq 0.35$ cm or PGA ≥ 80 Gal). A PGA value of 80 Gal in Taiwan equals a PGV value of 17 cm/s and seismic intensity of V, which is capable of causing minor damage, especially in the epicentral region (Wu et al., 2003). Unfortunately, the 2018 earthquake occurred during nighttime, so optimal utilization could not be achieved because most of these instruments are installed in schools. On the contrary, the 2019 earthquake occurred during the daytime, and most schools were vacated after the warning was issued successfully. Fig. 3 shows the lead-time (warning time) using PGA and PGV during the 2018 and 2019 earthquakes. The STA/LTA algorithm is used to pick the P-wave arrival on the event record. After the arrival time of the P-wave is confirmed, the P_d value is estimated using the initial few seconds of the record. Once P_d exceeds 0.35 cm, the warning is issued, and the warning time is marked as t_1. The embedded algorithm keeps on looking for the real PGA and PGV and marks their arrival as t_2. The lead-time is the difference between time t_2 and t_1. This lead-time is termed as real-time lead-time if the result is positive; otherwise, it is dropped. Each instrument provides a different lead-time using PGA and PGV. Generally, the lead-time using PGV is slightly longer than the PGA for the instruments close to the epicenter. The unilateral rupture and directivity effect may be the possible reason for this lead-time difference using different parameters. For this case, PGV may appear later than PGA. However, a mixed phenomenon is observed for the instruments placed away from the epicenter. During the 2018 earthquake, the lead-time for the instrument close to the epicenter (W011) was 1.1 s and 1.7 s, using PGA and PGV, respectively (Fig. 3a). Similarly, the lead-time for the closest instrument (W00E) during 2019 was 5.3 s and 7.6 s using PGA and PGV, respectively (Fig. 3b). It can be concluded that higher lead-time, at least a few seconds, maybe achieved using PGV for the instruments placed close to the epicenter in the blind zone, where the regional warning is not possible.

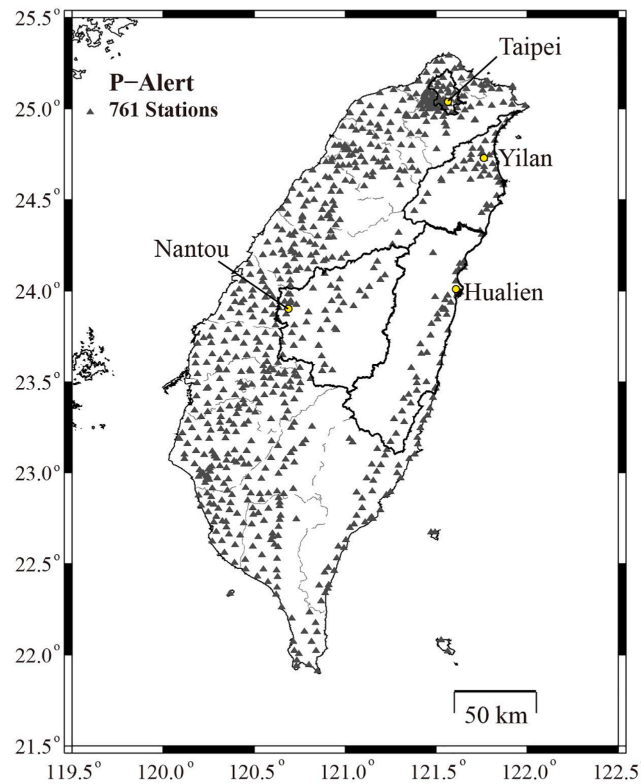

Fig. 2. Station distribution of P-Alert network in different parts of Taiwan. The whole region is densely instrumented except a few patches in the northeast direction of Taiwan, where proper logistics is not available.

Besides, data from each instrument in the field is regularly transferred to the central server stations at NTU and Institute of Earth Sciences, Academia Sinica, where data is routinely processed for the regional warning and the generation of shakemaps. The regional warning generated during each earthquake is used for research purposes, as CWB is the official agency for issuing a warning in Taiwan.

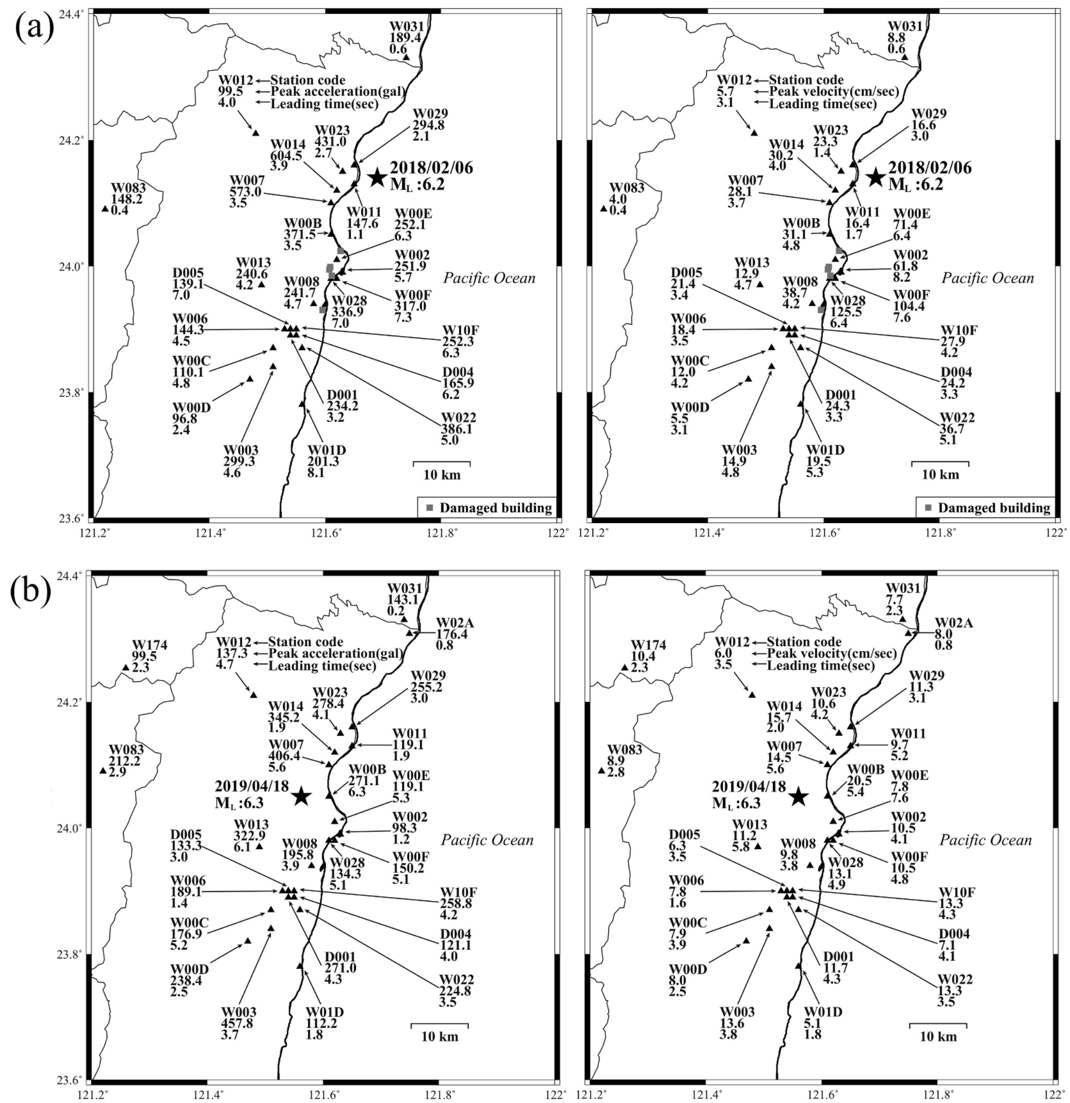

Fig. 3. The on-site PGA and PGV lead-time in the blind zone during the 2018 and 2019 earthquakes. (a) PGA and PGV lead-time during the 2018 earthquake. (b) PGA and PGV lead-time during the 2019 earthquake.

5. Shakemaps

A shakemap effectively assesses the damage pattern during an earthquake and provides situational awareness to disaster relief agencies to initiate a rapid response. In Taiwan, P-Alert starts generating shakemaps once 10–12 instruments confirm PGA to be 1.2 Gal. These shakemaps are delivered to concerned persons, including the National Science and Technology Center for Disaster Reduction, the nodal agency for relief work in Taiwan. These shakemaps are posted regularly on Facebook and are updated every 30 s.

During the 2018 earthquake, the shakemap triggered by 76 stations was posted on Facebook (https://www.facebook.com/Palert.Shakemap/) at 23:50:58 (about 17 s after earthquake occurrence) (Fig. 4a). The shakemap triggered by almost all 538 stations was available within 1.5 min (Fig. 4b). A total of 636 P-Alert instruments were installed when the 2018 earthquake occurred. The shakemap on Facebook was posted only with 538 instruments as some of the instruments recorded PGA less than 2.5 Gal and were not included in real-time plotting of PGA shakemaps. By the time the 2019 earthquake happened, there were 697 P-Alert instruments available on the whole island of Taiwan. The 2019 earthquake occurred at 13:01:9.9, and the PGA shakemap with the triggering of 93 stations was posted on Facebook at 13:01:22, approximately 15 s after the earthquake's origin (Fig. 4c). The complete shakemap with 627 instruments was available within 2 min of the occurrence of the earthquake (Fig. 4d). The PGA contours during the first shakemap are very strange, as only a few stations close to the epicenter have attained PGA values, especially towards the northwest and south directions. The final shakemap shows a different pattern, where smooth PGA contours can be observed in all directions, based on the data received by all 627 instruments. Some of the parts toward the south are not contoured because the instruments installed there recorded PGA less than 2.5 Gal.

In contrast to Fig. 4, showing the real-time PGA shakemaps, Figs. 5 and 6 illustrate the PGA and PGV shakemaps for 2018 and 2019 earthquakes using all the instruments (with those recorded PGA smaller than 2.5 Gal that excluded in the previous real-time shakemaps). The distance inverse interpolation scheme is used for interpolation, which has been well tested in earlier studies (Legendre et al., 2017; Mittal et al., 2018, 2019a; Wu et al., 2019; Yang et al., 2021, 2018). Different researchers (Worden et al., 2010, 2018) use different interpolation schemes, but interpolation established for P-Alert data is suitable for the present study (Yang et al., 2018). Though the shape of PGA contours for 2018 and 2019 earthquakes is the same in Figs. 4–6, the latter ones give smooth contours with proper demarcation and are easy to read the areas

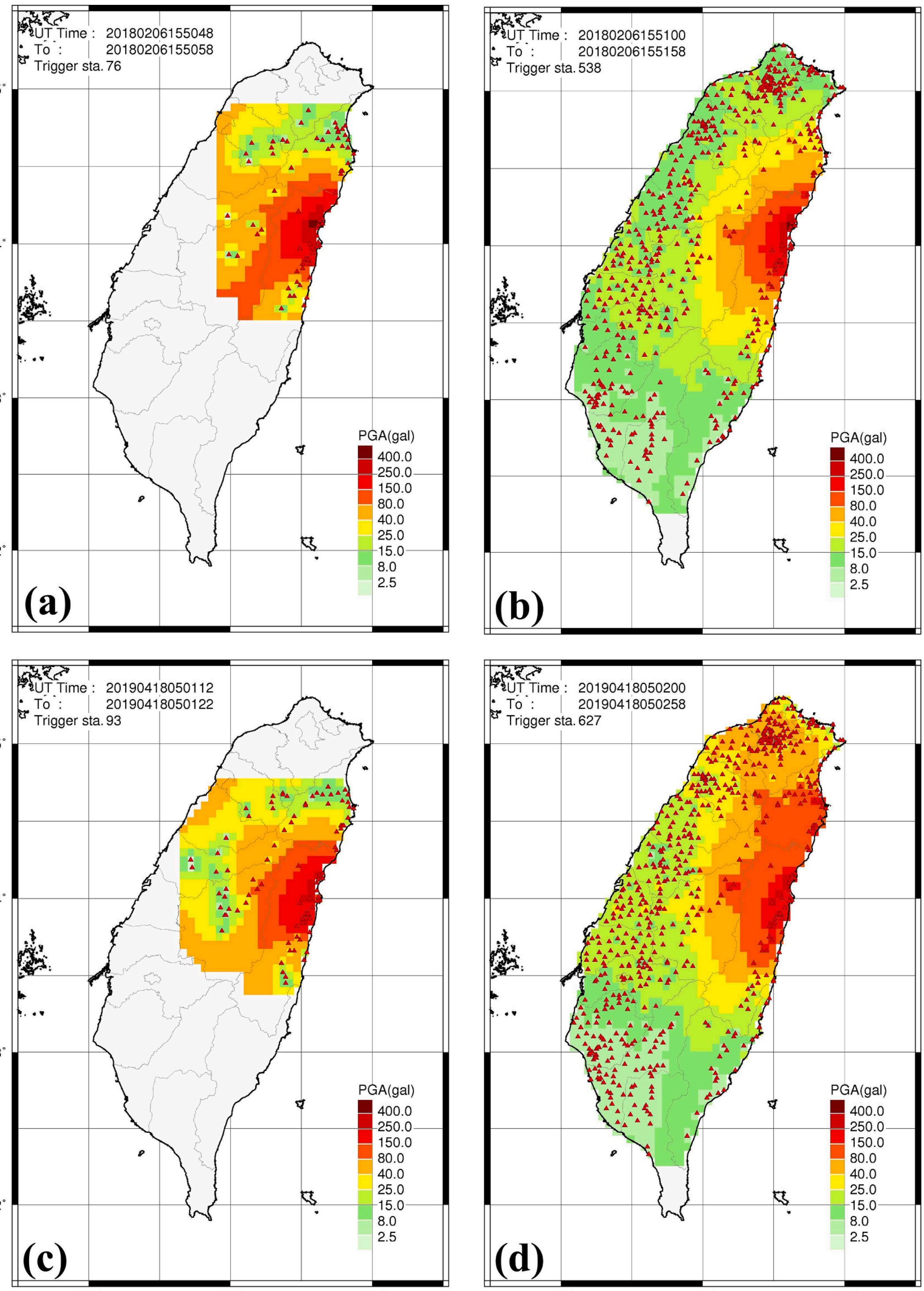

Fig. 4. The real-time peak ground acceleration maps for the 2018 and 2019 Hualien earthquakes. (a) The shakemap was triggered by 76 instruments during the 2018 earthquake. (b) The shakemap was posted 1.5 m later with the triggering of 538 instruments during the 2018 earthquake. (c) The shakemap posted 15 s after the occurrence of the 2019 Hualien earthquake with triggering 93 instruments. (d) The shakemap was posted on Facebook with the triggering of 627 instruments.

of different PGA values.

6. Discussions

The higher PGA values (> 400 Gal) were observed at a few stations in the epicentral region during the 2018 earthquake. The 400 Gal PGA contour is based on the data from nearly 4–5 instruments (Fig. 3a). The 250 Gal contour was extended in the epicentral region and the nearby Yilan area, based on data from nearly 12 instruments. More instruments could be recording these earthquakes if proper logistics (power supply and internet connection) were available (as Hualien is a mountainous area). A PGA value of 80 Gal in Taiwan equals PGV of 17 cm/s and seismic intensity of V, which is capable of causing minor damage, especially in the epicentral region (Wu et al., 2003). One can expect higher PGV contours (≥49 cm/s) corresponding to higher PGA contours (≥250 Gal). However, looking at the PGV contour map for this

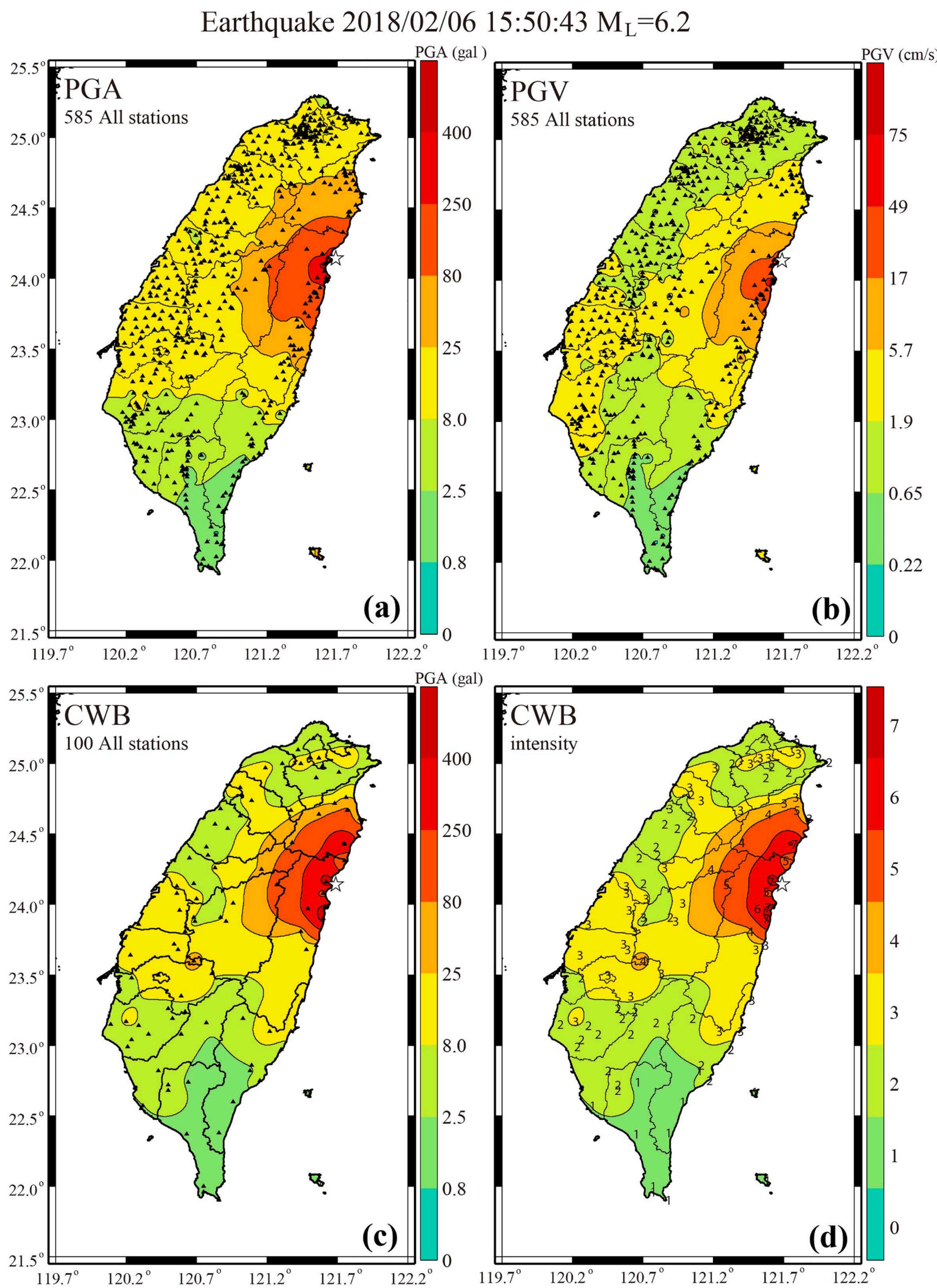

Fig. 5. Plotted PGA and PGV shakemap for the 2018 Hualien earthquake by including all the instruments that recorded PGA less than 2.5 Gal. (a) PGA shakemap, (b) PGV shakemap and, (c) PGA shakemap using the CWB network, (d) CWB intensity map, based on felt intensity and intensity drawn from PGA.

earthquake (Fig. 5b), a small contour of PGV $\geq$ 49 cm/s is observed, at the southwest of the epicenter closest to the Hualien where the Milun fault was ruptured, and the maximum destruction was caused (Yen et al. 2019). Considering the relation between PGA and PGV in Taiwan, this contour of PGV $\geq$ 49 cm/s (PGA $\geq$ 250 Gal) is expected in a broader region. The next observed contour is of PGV $\geq$ 17 cm/s. This contour of 17 cm/s encompasses the proximity of the Milun fault, where five buildings collapsed, causing 17 fatalities. Although higher PGA values were obtained in an extensive region, the destruction concentrated in a region with higher PGV values. So looking at the destruction caused by the earthquake and the shakemaps (PGA and PGV), the damage during this earthquake is closely related to PGV values.

During the 2019 earthquake, higher PGA values ($\geq$400 Gal) were recorded only at two stations. The 250 Gal contour encircles a small area and is smoothened using data from four instruments (Fig. 6a). The 80 Gal contour extends to the nearby regions of the epicenter. One of the basic differences between the 2018 and 2019 earthquakes is that the 25 Gal PGA contour of the 2019 event covered a larger area, including the

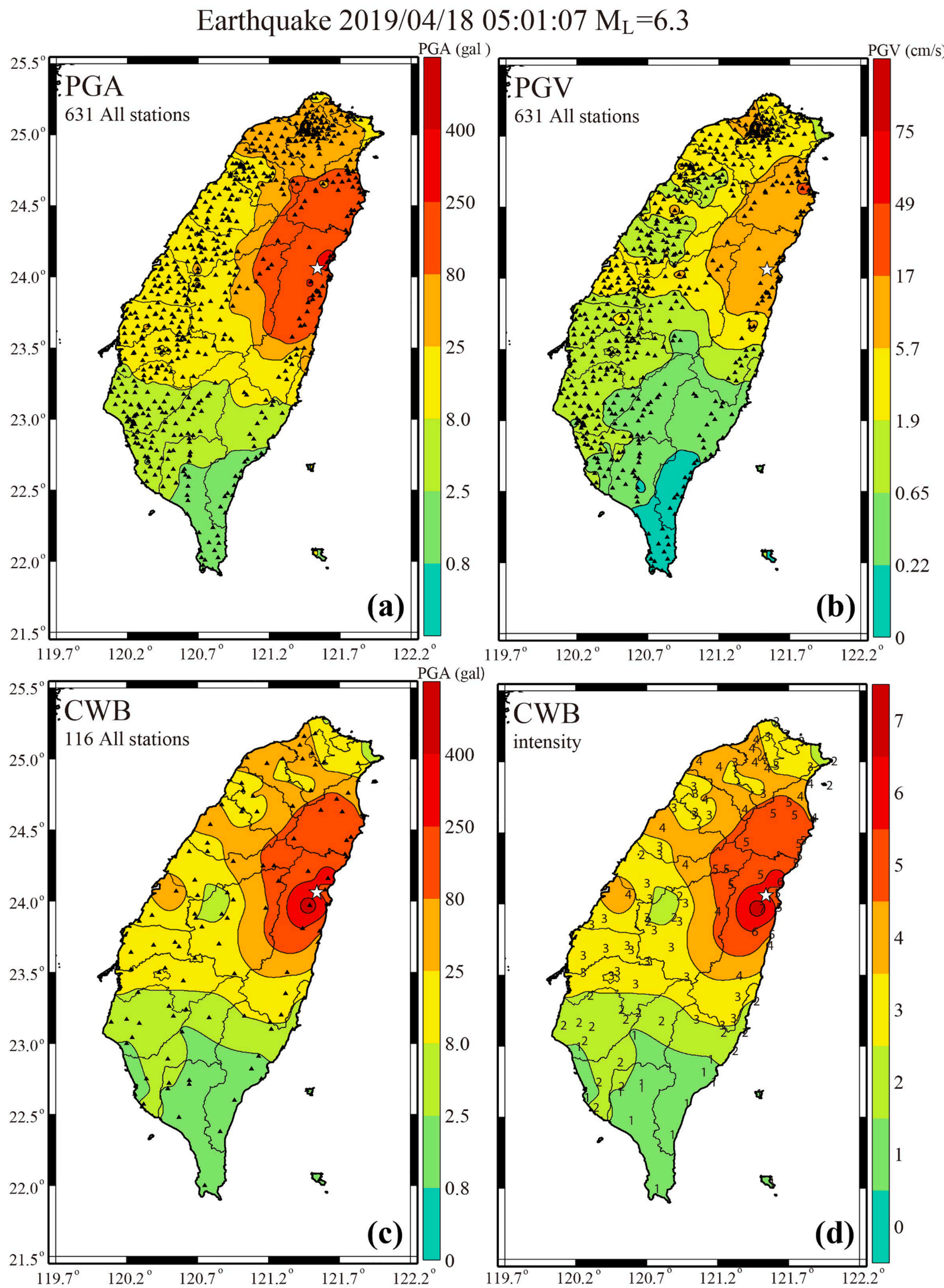

Fig. 6. Plotted PGA and PGV shakemap for the 2019 Hualien earthquake by including all the instruments that recorded PGA less than 2.5 Gal. (a) PGA, (b) PGV shakemap and, (c) PGA shakemap using the CWB network, (d) CWB intensity map, based on felt intensity and intensity drawn from PGA.

Taipei area, which was not observed during the 2018 earthquake. The simple reason for this observation may be the depth of the 2019 earthquake (18.8 km compared to the 10.0 km depth of the 2018 earthquake), which may have stimulated the nearby fault running in a northwest-southeast direction. Lee et al. (2020) proposed that the rapid northward rupture of the April 2019 earthquake caused a strong directivity effect coupled with the specific source radiation pattern, resulting in a large area of strong ground shaking in northern Taiwan. Also, the site effects played a major role in amplifying the ground shaking in the Yilan and Taipei areas. A higher PGV value (17 cm/s, corresponding to PGA of 80 Gal as per Wu et al., 2003) is found only at one station. Nevertheless, the PGV contour of 5.7 cm/s extends to a wider area in the epicentral region and Taipei (Fig. 6b). In Taipei, PGA values between 25 and 80 Gal were observed during this earthquake, which corresponds to 5.7–17.0 cm/s PGV contour. For such small PGA values in Taipei, no destruction is expected. However, a building in Taipei leaned against its neighbor after this earthquake, suggesting that the PGV scale correlates the destruction scenario better than the PGA does.

The CWB network uses sparse instrumentation (almost 120 real-time stations) to produce near real-time shakemaps and consumes more time in issuing the first report concerning shakemaps as compared to the P-Alert network. The CWB initially assigned M_L 6.0, and M_L 6.1 to 2018, and 2019 earthquakes, respectively. These magnitudes were subsequently revised to M_L 6.2 and M_L 6.3, respectively. Since the online instruments used by CWB are less than densely installed P-Alert network, the PGA shakemaps produced by the CWB network are relatively rough and sporadic, as shown in Figs. 5c and 6c. Only two or three instruments recorded the high PGA (0.4 g) values, and smooth contours are not attained because of the larger inter-station distance. Similarly, the 250 Gal contour in CWB shakemap is based on PGA values recorded by 3–4 instruments and may not reflect the correct PGA contour as more interpolation is required. On the contrary, the P-Alert network uses around twelve instruments to plot 250 Gal contour and is, therefore, smoother (Fig. 3a). Wu et al. (2019) summarized the difference between P-Alert and CWB PGA shakemaps for the 2018 earthquake. Fig. 6c shows the plotted PGA shakemaps for the 2019 earthquake using PGA values from 116 instruments for the CWB network. The highest PGA contour ($\geq$400 Gal) towards the southwest of the epicenter is based on the data from a single instrument. It may not be authentic as no other instrument is found in the neighborhood to check how PGA values decrease. The 250 Gal contour using a high degree of interpolation extends to a wider area based on data from three instruments. The P-Alert network also plotted this 250 Gal contour based on data from four instruments, but the other instruments recording PGA less than 250 Gal were in the proximity to verify the trend of contour. The 25 Gal contour using the CWB network is observed irregularly in different parts, including Taipei. This 25 Gal contour using the P-Alert network is based on the data recorded by around 150 instruments. Also, the CWB network lacks in producing PGV shakemaps, which are essential for demarcating the areas of significant damage, as described above. Figs. 5d and 6d represent the CWB intensity maps for two earthquakes, based on felt intensity and intensity drawn from PGA.

Data generated using the dense network efficiently finds the rupture direction, a significant parameter in assessing the damage pattern. The station in the forward direction of the rupture will record higher PGV values as compared to the stations placed in the opposite direction. The rupture direction is well observed during both the 2018 and 2019 earthquakes, where higher PGV values are obtained in southwest and northeast directions, respectively (Fig. 7). Assessing rupture directivity using P-Alert has been well documented in many studies previously (Hsieh et al., 2014; Jan et al., 2018; Wu et al., 2016, 2019).

7. Conclusions

The performance of the P-Alert network in the Hualien area of Taiwan is evaluated in terms of EEW warning (on-site as well as regional), and plotting PGA and PGV shakemaps, using the data of two moderate earthquakes that occurred in 2018 and 2019.

During both the earthquakes, higher lead times using PGV were reported at nearby instruments than the farther instruments. For all other instruments, the lead-time using PGA and PGV shows a mixed pattern. During both earthquakes, slightly higher lead times were observed at instruments close to the epicenter; the EEW using PGV might be a better option for the instruments situated in the blind zone.

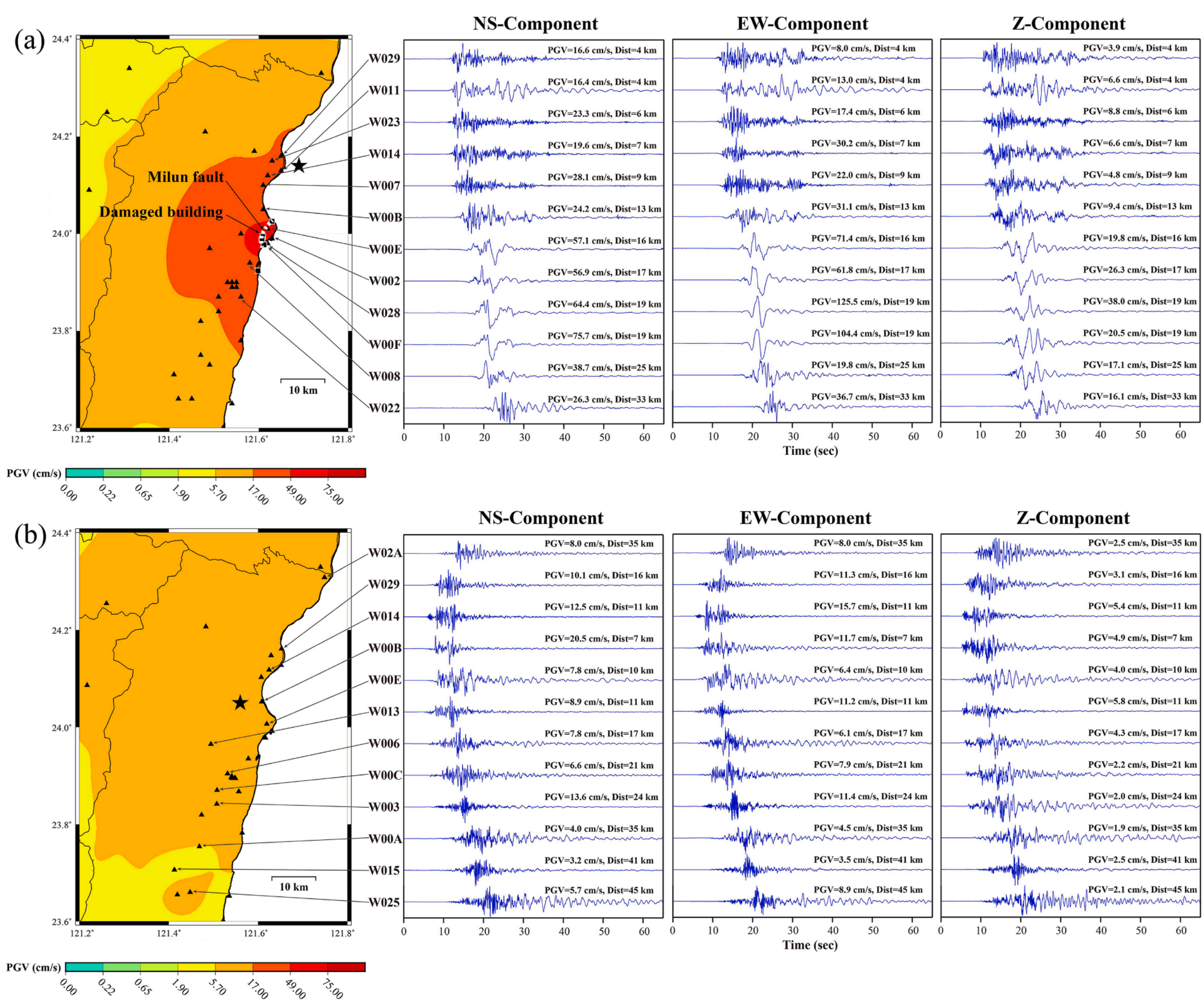

Fig. 7. Quality of data recorded by the P-Alert instruments during the 2018 earthquake (a) and the 2019 earthquake (b).

The higher PGV values of the order of 49 cm/s (corresponding to a PGA value of 250 Gal) were observed at one station during the 2018 earthquake. The other observed PGV contour is about 17 cm/s during the 2018 earthquake in the epicentral region, where maximum destruction was caused. This higher PGV value (17 cm/s) during 2019 was observed only at one station, towards the northeast of the epicenter. Another PGV (5.7 cm/s, corresponding to 25 Gal, capable of causing light damage in weak houses) contour surrounded a wider area during the 2019 earthquake (including Taipei) as compared to the 2018 earthquake (where PGV contour was in the surrounding areas of the epicenter). For such a higher PGA value perceived during both earthquakes, one would expect severe damage in the epicentral region. The 2018 earthquake caused heavy destruction in the epicentral region, including 17 fatalities; however, the 2019 earthquake caused very negligible damage in the epicentral region and Taipei. One building in Taipei leaned against its neighbor after shifting its foundation, during the 2019 earthquake. The obvious difference in demolition caused during the two earthquakes can be observed from PGV shakemaps. The maximum loss during the 2018 earthquake was caused in an area encircling higher PGV values ($\geq$17 cm/s). The light damage (minor/negligible damage in buildings) during both earthquakes was observed in areas having a PGV value of 5.7 cm/s. From here, it can be concluded that the PGV shakemaps (at least during these two earthquakes) may portray a better picture of damage distribution in an area as compared to PGA shakemaps.

CRediT authorship contribution statement

Himanshu Mittal: Methodology, Investigation, Writing – original draft. **Benjamin Ming Yang:** Methodology, Software, Validation, Investigation. **Tai-Lin Tseng:** Investigation, Supervision. **Yih-Min Wu:** Conceptualization, Methodology, Validation, Writing – review & editing, Supervision.

Declaration of Competing Interest

The authors declare that they have no known competing financial interests or personal relationships that could have appeared to influence the work reported in this paper.

Data availability statement

The strong motion waveform records from the P-Alert network used in this study can be downloaded at http://palert.earth.sinica.edu.tw/db/.

Acknowledgment

The authors gratefully acknowledge the Ministry of Science and Technology (MOST), Taiwan to sponsor the project, under which this study was carried out. The Research Center of Future Earth of the National Taiwan University (NTU) also supported our work. The GMT software from Wessel and Smith (1998) was used in plotting most of the Figures and is gratefully acknowledged. The constructive comments from Dr. Sanjay Singh Bora, one anonymous reviewer, Associate Editor (Dr. Gahalaut), and Miss Diane Chung helped in shaping the manuscript.

Appendix A. Supplementary material

Supplementary data to this article can be found online at https://doi.org/10.1016/j.jseaes.2021.104936.

References

Chen, D.-Y., Hsiao, N.-C., Wu, Y.-M., 2015. The earthworm based earthquake alarm reporting system in Taiwan. Bull. Seismol. Soc. Am. 105 (2A), 568–579. https://doi.org/10.1785/0120140147.

Chen, D.Y., Wu, Y.M., Chin, T.L., 2017. An empirical evolutionary magnitude estimation for early warning of earthquakes. J. Asian Earth Sci. 135, 190–197. https://doi.org/10.1016/j.jseaes.2016.12.028.

Hsieh, C.Y., Wu, Y.M., Chin, T.L., Kuo, K.H., Chen, D.Y., Wang, K.S., Chan, Y.T., Chang, W.Y., Li, W.S., Ker, S.H., 2014. Low cost seismic network practical applications for producing quick shaking maps in Taiwan. Terr. Atmos. Ocean. Sci. 25, 617–624. https://doi.org/10.3319/TAO.2014.03.27.01(T).

Hsu, T.Y., Lin, P.Y., Wang, H.H., Chiang, H.W., Chang, Y.W., Kuo, C.H., Lin, C.M., Wen, K.L., 2018. Comparing the performance of the NEEWS earthquake early warning system against the CWB system during the 6 February 2018 Mw 6.2 Hualien Earthquake. Geophys. Res. Lett. 45, 6001–6007. https://doi.org/10.1029/2018GL078079.

Jan, J.C., Huang, H.-H., Wu, Y.-M., Chen, C.-C., Lin, C.-H., 2018. Near-real-time estimates on earthquake rupture directivity using near-field ground motion data from a dense low-cost seismic network. Geophys. Res. Lett. 45 (15), 7496–7503. https://doi.org/10.1029/2018GL078262.

Koulakov, I., Wu, Y.M., Huang, H.H., Dobretsov, N., Jakovlev, A., Zabelina, I., Jaxybulatov, K., Chervov, V., 2014. Slab interactions in the Taiwan region based on the P- and S-velocity distributions in the upper mantle. J. Asian Earth Sci. 79, 53–64. https://doi.org/10.1016/j.jseaes.2013.09.026.

Kumar, A., Mittal, H., Chamoli, B., Gairola, A., Jakka, R.S., Srivastava Amit, 2014. Earthquake Early Warning System for Northern India. 15th SEE-2014.

Kumar, S., Mittal, H., Roy, K.S., Wu, Y.M., Chaubey, R., Singh, A.P., 2020. Development of earthquake early warning system for Kachchh, Gujarat, in India using τc and P d. Arab. J. Geosci. 13 (14), 1–11. https://doi.org/10.1007/s12517-020-05353-3.

Lee, S.J., Wong, T.P., Liu, T.Y., Lin, T.C., Chen, C.T., 2020. Strong ground motion over a large area in northern Taiwan caused by the northward rupture directivity of the 2019 Hualien earthquake. J. Asian Earth Sci. 192 https://doi.org/10.1016/j.jseaes.2019.104095.

Legendre, C.P., Tseng, T.L., Mittal, H., Hsu, C.-H., Karakhanyan, A., Huang, B.S., 2017. Complex wave propagation revealed by peak ground velocity maps in the Caucasus Area. Seismol. Res. Lett. 88 (3), 812–821. https://doi.org/10.1785/0220160178.

Lin, J.-L., Kuo, C.-H., Chang, Y.-W., Chao, S.-H., Li, Y.-A., Shen, W.-C., Yu, C.-H., Yang, C.-Y., Lin, F.-R., Hung, H.-H., Chen, C.-C., Su, C.-K., Hsu, S.-Y., Lu, C.-C., Chung, L.-L., Hwang, S.-J., 2020. Reconnaissance and learning after the February 6, 2018, earthquake in Hualien, Taiwan. Bull. Earthquake Eng. 18 (10), 4725–4754.

Ma, K.F., Wu, Y.M., 2019. Preface to the focus section on the 6 February 2018 M w 6.4 Hualien, Taiwan, earthquake. Seismol. Res. Lett. 90, 15–18. https://doi.org/10.1785/0220180356.

Mittal, H., Kumar, A., Kumar, A., Kumar, R., 2015. Analysis of ground motion in Delhi from earthquakes recorded by strong motion network. Arab. J. Geosci. 8 (4), 2005–2017. https://doi.org/10.1007/s12517-014-1357-3.

Mittal, H., Kumar, A., Wu, Y.M., Kamal, Kumar, A., 2016. Source study of Mw5.4 April 4, 2011 India-Nepal border earthquake and scenario events in the Kumaon-Garhwal Region. Arab. J. Geosci. 9 https://doi.org/10.1007/s12517-016-2330-0.

Mittal, Himanshu, Wu, Yih-Min, Lin, Ting-Li, Legendre, Cédric P., Gupta, Sushil, Yang, Benjamin M., 2019a. Time-dependent shake map for Uttarakhand Himalayas, India, using recorded earthquakes. Acta Geophys. 67 (3), 753–763. https://doi.org/10.1007/s11600-019-00281-7.

Mittal, Himanshu, Wu, Yih-Min, Sharma, Mukat Lal, Yang, Benjamin Ming, Gupta, Sushil, 2019b. Testing the performance of earthquake early warning system in northern India. Acta Geophys. 67 (1), 59–75. https://doi.org/10.1007/s11600-018-0210-6.

Mittal, H., Wu, Y.M., Sharma, M.L., Lin, T.L., Yang, B.M., 2018. Shake maps generation for Delhi region using two different algorithms. In 16th symposium on earthquake engineering, Indian Institute of Technology, Roorkee, Dec. 20-22, Paper No. 232.

Shyu, J.B.H., Chen, C.F., Wu, Y.M., 2016. Seismotectonic characteristics of the northernmost Longitudinal Valley, eastern Taiwan: structural development of a vanishing suture. Tectonophysics 692, 295–308. https://doi.org/10.1016/j.tecto.2015.12.026.

Shyu, J.B.H., Sieh, K., Chen, Y.G., Liu, C.S., 2005. Neotectonic architecture of Taiwan and its implications for future large earthquakes. J. Geophys. Res. Solid Earth 110, B08402. https://doi.org/10.1029/2004JB003251.

Shyu, J. Bruce H., Wu, Yih-Min, Chang, Chien-Hsin, Huang, Hsin-Hua, 2011. Tectonic erosion and the removal of forearc lithosphere during arc-continent collision: evidence from recent earthquake sequences and tomography results in eastern Taiwan. J. Asian Earth Sci. 42 (3), 415–422. https://doi.org/10.1016/j.jseaes.2011.05.015.

Wang, K.S., Mittal, H., Wu, Y.M., Chao, W.A., 2018. Building effects on the p-alert-based real-time shaking map determination. Seismol. Res. Lett. 89, 2314–2321. https://doi.org/10.1785/0220170252.

Wessel, P., Smith, W.H.F., 1998. New, improved version of generic mapping tools released. Eos, Trans. Am. Geophys. Union. https://doi.org/10.1029/98EO00426.

Worden, C.B., Thompson, E.M., Baker, J.W., Bradley, B.A., Luco, N., Wald, D.J., 2018. Spatial and spectral interpolation of ground-motion intensity measure observations. Bull. Seismol. Soc. Am. 108, 866–875. https://doi.org/10.1785/0120170201.

Worden, C.B., Wald, D.J., Allen, T.I., Lin, K., Garcia, D., Cua, G., 2010. A revised ground-motion and intensity interpolation scheme for shakemap. Bull. Seismol. Soc. Am. 100, 3083–3096. https://doi.org/10.1785/0120100101.

Wu, Y.M., Lin, T.L., 2014. A Test of Earthquake Early Warning System Using Low Cost Accelerometer in Hualien, Taiwan. https://doi.org/10.1007/978-3-642-12233-0_13.

Wu, Y.M., Liang, W.T., Mittal, H., Chao, W.A., Lin, C.H., Huang, B.S., Lin, C.M., 2016. Performance of a Low-Cost Earthquake Early Warning System (P -Alert) during the 2016 M_L 6.4 Meinong (Taiwan) Earthquake. Seismol. Res. Lett. 87, 1050–1059. https://doi.org/10.1785/0220160058.

Wu, Y.M., Mittal, H., Huang, T.C., Yang, B.M., Jan, J.C., Chen, S.K., 2019. Performance of a Low-Cost Earthquake Early Warning System (P-Alert) and Shake Map Production during the 2018 Mw 6.4 Hualien, Taiwan. Earthquake. Seismol. Res. Lett. 90, 19–29. https://doi.org/10.1785/0220180170.

Wu, Yih-Min, 2015. Progress on development of an earthquake early warning system using low-cost sensors. Pure Appl. Geophys. 172 (9), 2343–2351. https://doi.org/10.1007/s00024-014-0933-5.

Wu, Y.-M., Chen, D.-Y., Lin, T.-L., Hsieh, C.-Y., Chin, T.-L., Chang, W.-Y., Li, W.-S., Ker, S.-H., 2013. A high-density seismic network for earthquake early warning in Taiwan based on low cost sensors. Seismol. Res. Lett. 84 (6), 1048–1054. https://doi.org/10.1785/0220130085.

Wu, Y.M., Chung, J.K., Shin, T.C., Hsiao, N.C., Tsai, Y.B., Lee, W.H.K., Teng, T.L., 1999. Development of an integrated earthquake early warning system in Taiwan - Case for the Hualien area earthquakes. Terr. Atmos. Ocean. Sci. 10, 719–736. https://doi.org/10.3319/TAO.1999.10.4.719(T).

Wu, Y.M., Hsiao, N.C., Teng, T.L., 2004. Relationships between strong ground motion peak values and seismic loss during 1999 Chi-Chi, Taiwan Earthquake. Nat. Hazards 32, 357–373. https://doi.org/10.1023/B:NHAZ.0000035550.36929.d0.

Wu, Y.M., Hsiao, N.C., Teng, T.L., Shin, T.C., 2002. Near real-time seismic damage assessment of the rapid reporting system. Terr. Atmos. Ocean. Sci. 13, 313–324. https://doi.org/10.3319/TAO.2002.13.3.313(CCE).

Wu, Y.M., Shin, T.C., Chen, C.C., Tsai, Y.B., Lee, W.H.K., Teng, T.L., 1997. Taiwan rapid earthquake information release system. Seismol. Res. Lett. 68, 931–943. https://doi.org/10.1785/gssrl.68.6.931.

Wu, Y.M., Shin, T.C., Tsai, Y.B., 1998. Quick and reliable determination of magnitude for seismic early warning. Bull. Seismol. Soc. Am. 88, 1254–1259.

Wu, Y.M., Teng, T.L., 2002. A virtual subnetwork approach to earthquake early warning. Bull. Seismol. Soc. Am. 92, 2008–2018. https://doi.org/10.1785/0120010217.

Wu, Y.M., Teng, T.L., Shin, T.C., Hsiao, N.C., 2003. Relationship between peak ground acceleration, peak ground velocity, and intensity in Taiwan. Bull. Seismol. Soc. Am. 93, 386–396. https://doi.org/10.1785/0120020097.

Yang, B.M., Huang, T.C., Wu, Y.M., 2018. Shakingalarm: A nontraditional regional earthquake early warning system based on time-dependent anisotropic peak ground-motion attenuation relationships. Bull. Seismol. Soc. Am. 108, 1219–1230. https://doi.org/10.1785/0120170105.

Yang, B.M., Mittal, H., Wu, Y.M., 2021. Real-time production of PGA, PGV, intensity, and sa shakemaps using dense mems-based sensors in Taiwan. Sensors 21, 943. https://doi.org/10.3390/s21030943.

Yen, J.Y., Lu, C.H., Dorsey, R.J., Kuo-Chen, H., Chang, C.P., Wang, C.C., Chuang, R.Y., Kuo, Y.T., Chiu, C.Y., Chang, Y.H., Bovenga, F., Chang, W.Y., 2019. Insights into seismogenic deformation during the 2018 Hualien, Taiwan, earthquake sequence from InSAR, GPS, and modeling. Seismol. Res. Lett. 90, 78–87. https://doi.org/10.1785/0220180228.

Yu, Shui-Beih, Chen, Horng-Yue, Kuo, Long-Chen, 1997. Velocity field of GPS stations in the Taiwan area. Tectonophysics 274 (1-3), 41–59. https://doi.org/10.1016/S0040-1951(96)00297-1.